Title
Pathological alterations involve the entire skin physiological milieu in infantile and early-childhood port-wine stain

Journal
British Journal of Dermatology, 177(1)

ISSN
0007-0963

Authors
Tan, W
Zakka, LR
Gao, L
et al.

Publication Date
2017-07-01

DOI
10.1111/bjd.15068

Peer reviewed

HHS Public Access

Author manuscript

Br J Dermatol. Author manuscript; available in PMC 2018 July 01.

Published in final edited form as:

Br J Dermatol. 2017 July ; 177(1): 293–296. doi:10.1111/bjd.15068.

Pathological Alterations Involve the Entire Skin Physiological Milieu in Infantile and Early Childhood Port Wine Stain

W. Tan[1,*], **L.R. Zakka**[2], **L. Gao**[1,3], **J. Wang**[1,5], **F. Zhou**[1,5], **M.K. Selig**[6], **R. Anvari**[1], **A. Sukanthanag**[1], **G. Wang**[4], **M.C. Mihm Jr**[2], and **J.S. Nelson**[1,4]

[1]Department of Surgery, Beckman Laser Institute and Medical Clinic, University of California, Irvine, Irvine, California 92617, USA

[2]Department of Dermatology, Brigham and Women's Hospital, Harvard Medical School, Boston, Massachusetts 02115, USA

[3]Department of Dermatology, Xijing Hospital, Fourth Military Medical University, Xi'an, 710032, China

[4]Department of Biomedical Engineering, University of California, Irvine, Irvine, California 92617, USA

[5]The Third Xiangya Hospital, Xiangya School of Medicine, Central South University, Changsha, Hunan, 412000, China

[6]Department of Pathology, Massachusetts General Hospital, Harvard Medical School, Boston, Massachusetts 02114, USA

To the editor

Port wine stain (PWS) is a congenital vascular malformation of human skin involving the superficial vascular plexus, occurring in an estimated 3–5 children per 1,000 live births.[1] Understanding the pathogenesis of PWS in infant skin is critical for improving therapeutic outcome but to date has been incompletely understood. The study was approved by the Institutional Review Board at the University of California, Irvine. One infant and one young child with PWS were enrolled in this study. One was a 9-month-old female and the other was a 22-month-old male. Punch biopsies (3 mm) from a selected PWS site and adjacent normal skin were taken for comparison from the same subjects for this study.

In both patients, normal skin blood vessels were observed to have an average diameter of 15 μm, while the PWS blood vessels in the dermis were enlarged with variable diameters up to 85 μm at similar depths (Figures 1a, b). On transmission electron microscopy (TEM), normal vessels exhibited prominent endothelial cells (ECs) with minimal thickening of the basement membrane and pericytes abutting the basement membrane zone (Figure 1c). In

Correspondence: Wenbin Tan, Department of Surgery, Beckman Laser Institute and Medical Clinic, University of California, Irvine, Irvine, California 92617, USA. wenbint@uci.edu Phone: 949-824-3754 Fax: 949-824-6969.

Financial Disclosure: None declared.

PWS vessels, there was a striking increase in the number of layers of both pericytes and basement membranes, resulting in a thickened blood vessel wall (Figure 1d). The PWS vessels exhibited very cellular thickened perivascular spaces with apparent fibrosis and entrapment of the pericytes (Figure 1d). There was excessive duplication of the basal laminae surrounding PWS vessels (Figure 1d). These laminae had irregular shapes and entrapped pericytes. In the PWS blood vessels, there was prominent hob-nailing of the ECs with striking gaps between the ECs, bulging into the lumen (Figure 1e). Attachment plaques between ECs noted in the normal control blood vessels (Figure 1f) were absent in the PWS vessels (Figure 1e).

Immunohistochemistry staining with smooth muscle actin (SMA) antibody showed its expression was defective in the pericytes of PWS blood vessels as compared to normal control blood vessels with similar sizes from the same subjects (Figures 1g, h). TEM examination of smooth muscle showed multiple degenerative changes (Figure 1i). There were abnormal shapes of the muscle, cytoplasmic vacuoles and amorphous debris separating muscular fibers (Figure 1j).

We observed the enlargement of elastic fibers associated with hypertrophic collagen fibers in PWS skin (Figure 2a). The collagen fibers showed an increase in their diameters in PWS skin as compared to the normal control skin at a similar depth in the skin (Figure 2b). TEM exhibited prominent thickened collagen bundles (Figure 2c) and disorganized elastic fibers (Figure 2d). Verhoeff-Van Gieson stain showed numerous hypertrophied collagen and elastic fibers near PWS blood vessels, which were consistent with the TEM findings. There were no hypertrophied collagen fibers observed adjacent to normal control blood vessels (Figures 2e,f). Collagen fibers exhibited a more anisotropic arrangement (orientation dependent) in PWS skin but an isotropic orientation (uniformity in all orientations) in the normal control skin (Figures 2g,h).

We then measured the cross sectional area (μm^2) of collagen bundles from semi-thin sections. We found 69.6% of collagen bundles had a cross sectional area less than 10 μm^2, and 30.4% from 10–70 μm^2 in the normal control skin. In PWS skin, we found 32.3% of collagen bundles had a cross sectional area less than 10 μm^2, 51.0% from 10–70 μm^2, and 16.7% greater than 70μm^2 (Figure 2i). A much greater percentage of collagen bundles showed enlargement (>20 μm^2) in PWS skin (48.9%) as compared to normal control skin (12.6%). The data could be fit into an exponential decay curve. We next measured the coherent index to evaluate the orientation orders and isotropy of collagen bundles. Both data showed a Gaussian distribution. Only 3% of the collagen bundles in the normal control skin exhibited coherent indexes from 0.6 to 0.7, but 19.3% in PWS skin fell into the same coherent index ranges (Figure 2j), suggesting a considerable portion of collagen bundles in PWS skin showed a more anisotropic pattern. There are more than 10 distinct types of collagens found in human skin.[2] Any impairment during collagen synthesis and assembly may cause these abnormalities. Therefore, the hypertrophied collagen fibers may result from the aggregation or polymerization of an excessive quantity of collagen precursors or fragments synthesized locally.

In this study, we have found that thickening of vessel walls is a common and predominant feature in both PWS subjects. Proliferation of pericytes, duplicate layers of basal laminae, and the deposition of loosely arrayed single collagen fibers in the midst of proteinaceous debris all contribute to PWS vessel wall thickening. Also, the abnormality of SMA of pericytes suggests a deficiency of perivascular support may be another factor leading to the progressive dilatation of PWS blood vessels. Many small vessels showed multiple layers of basement membranes without significant ectasia in both cases. These abnormalities of PWS vessel walls are the pathological alterations that occur first prior to the dilatation of the blood vessels.

The role of genetic mutations must also be considered in order to explain some of the abnormalities detected in this study. Recently, a sporadic somatic mutation (R183Q) in guanine nucleotide-binding protein, G alpha subunit q (GNAQ) has been identified in PWS lesions,[3, 4] and is enriched in PWS blood vessels.[5, 6] In our previous report, the GNAQ mutation had been identified to be present in the blood vessels, connective tissues, hair follicles/glands in the PWS skin from these two subjects.[6] Our results indicate that perivascular pluripotent cells, which can give rise to multi-lineages[7, 8], may harbor with GNAQ (R183Q) in PWS[6] and account for the multiple pathologies observed in blood vessels, stroma, smooth muscle and extracellular matrix components in both subjects. Moreover, many other somatic mutations have also been reported in PWS, including phosphatidylinositol 3-kinase, *EPHA3, c-Myb*, and *Beta Platelet-derived Growth Factor Receptor*.[4, 9] Mutations in these genes may lead to some of the morphological abnormalities seen in our current study. Finally, we have shown that extracellular signal-regulated kinases and c-Jun N-terminal protein kinases were the first to be activated in these young subjects[10], possibly contributing to the early pathological progression of PWS seen in this study.

In summary, our findings show that there are multiple pathological abnormalities present very early on in PWS infantile and early childhood skin, including an increase in the number of layers of both pericytes and basement membranes, degenerative smooth muscles, disorganized and hypertrophy of collagen and elastic fibers. These findings suggest PWS is not only a vascular malformation, but also a disorder involving the entire physiological milieu of human skin, which is present in infants and young children.

Acknowledgments

We greatly appreciate the Sue & Bill Gross Stem Cell Research Center at the University of California, Irvine, for their assistance with the histology image acquiring process experiments. Institutional support was provided by the Arnold and Mabel Beckman Foundation and the David and Lucile Packard Foundation.

Funding/Support: This study was supported in part by NIH AR063766 to WT, AR59244 to JSN, and the American Society for Laser Medicine and Surgery research grant F03.12 and F01.13 to WT.

REFERENCES

1. Mulligan PR, Prajapati HJ, Martin LG, et al. Vascular anomalies: classification, imaging characteristics and implications for interventional radiology treatment approaches. Br J Radiol. 2014; 87:20130392. [PubMed: 24588666]
2. Kivirikko KI. Collagens and their abnormalities in a wide spectrum of diseases. Ann Med. 1993; 25:113–126. [PubMed: 8387797]

3. Shirley MD, Tang H, Gallione CJ, et al. Sturge-Weber Syndrome and Port-Wine Stains Caused by Somatic Mutation in GNAQ. N Engl J Med. 2013; 368:1971–1979. [PubMed: 23656586]
4. Lian CG, Sholl LM, Zakka LR, et al. Novel Genetic Mutations in a Sporadic Port-Wine Stain. JAMA Dermatol. 2014; 150:1336–1340. [PubMed: 25188413]
5. Couto JA, Huang L, Vivero MP, et al. Endothelial Cells from Capillary Malformations Are Enriched for Somatic GNAQ Mutations. Plast Reconstr Surg. 2016; 137:77e–82e.
6. Tan W, Nadora DM, Gao L, et al. The somatic GNAQ mutation (R183Q) is primarily located in Port Wine Stain blood vessels. J Am Acad Dermatol. 2016; 74:380–383. [PubMed: 26775782]
7. Arbiser JL, Raab G, Rohan RM, et al. Isolation of mouse stromal cells associated with a human tumor using differential diphtheria toxin sensitivity. Am J Pathol. 1999; 155:723–729. [PubMed: 10487830]
8. Arbiser JL, Yeung R, Weiss SW, et al. The generation and characterization of a cell line derived from a sporadic renal angiomyolipoma: use of telomerase to obtain stable populations of cells from benign neoplasms. Am J Pathol. 2001; 159:483–491. [PubMed: 11485907]
9. Luks VL, Kamitaki N, Vivero MP, et al. Lymphatic and other vascular malformative/overgrowth disorders are caused by somatic mutations in PIK3CA. J Pediatr. 2015; 166:1048–1054. e1–e5. [PubMed: 25681199]
10. Tan W, Chernova M, Gao L, et al. Sustained activation of c-Jun N-terminal and extracellular signal-regulated kinases in port-wine stain blood vessels. J Am Acad Dermatol. 2014; 71:964–968. [PubMed: 25135651]

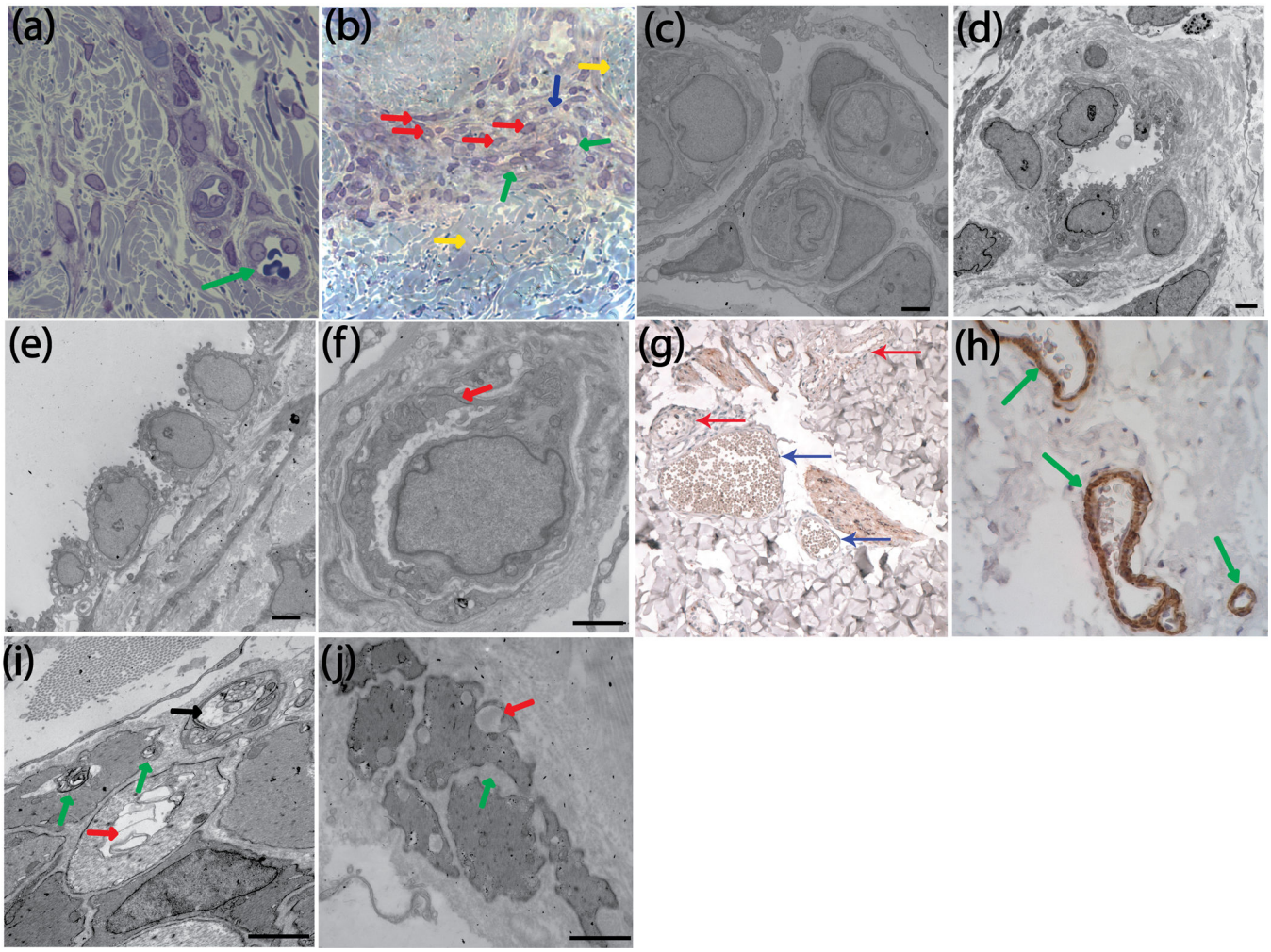

Figure 1.

Abnormalities of post-capillary venule-like blood vessels and increase in pericyte layers in infantile and early childhood PWS. (a) Normal blood vessels (green arrow) in the control skin. (b) A blood vessel with duplication of basement membranes (green arrows), marked thickening of the wall (blue arrow), and increased pericytes (red arrows), all surrounded by hypertrophied collagen fibers (yellow arrows). Giemsa stain (300×). (c) TEM showing normal capillary venular structure of the superficial plexus with pericytes abutting ECs. (d) Prominent PWS ECs with numerous cytoplasmic vesicles, duplication of the basal lamina, scattered amorphous debris, and single collagen fibers. (e) PWS ECs with marked hob-nailing are associated with prominent reduplication of the basal lamina. The connective tissue appeared abnormally fragmented. (f) A normal EC with normal attachment plaque (white arrow). (g) Dilated PWS blood vessel exhibited a deficiency in expression of SMA in pericytes (Red and Blue arrows). (h) Strong expression level of SMA was found in the normal cutaneous blood vessels (green arrows). (200×). (i) Degeneration of muscle fibers with the large lacunae present in the cytoplasm (red arrow), as well as lucent bodies containing debris (green arrows). There were myelin structures (black arrow). (j) TEM image showing marked abnormality of smooth muscle. There were intracytoplasmic

vacuoles (red arrow) and separation of fibers by amorphous material (green arrow). Scale bar: 2 μm; (a)-(c): 22-month-old male; (d)-(j):9-month-old female.

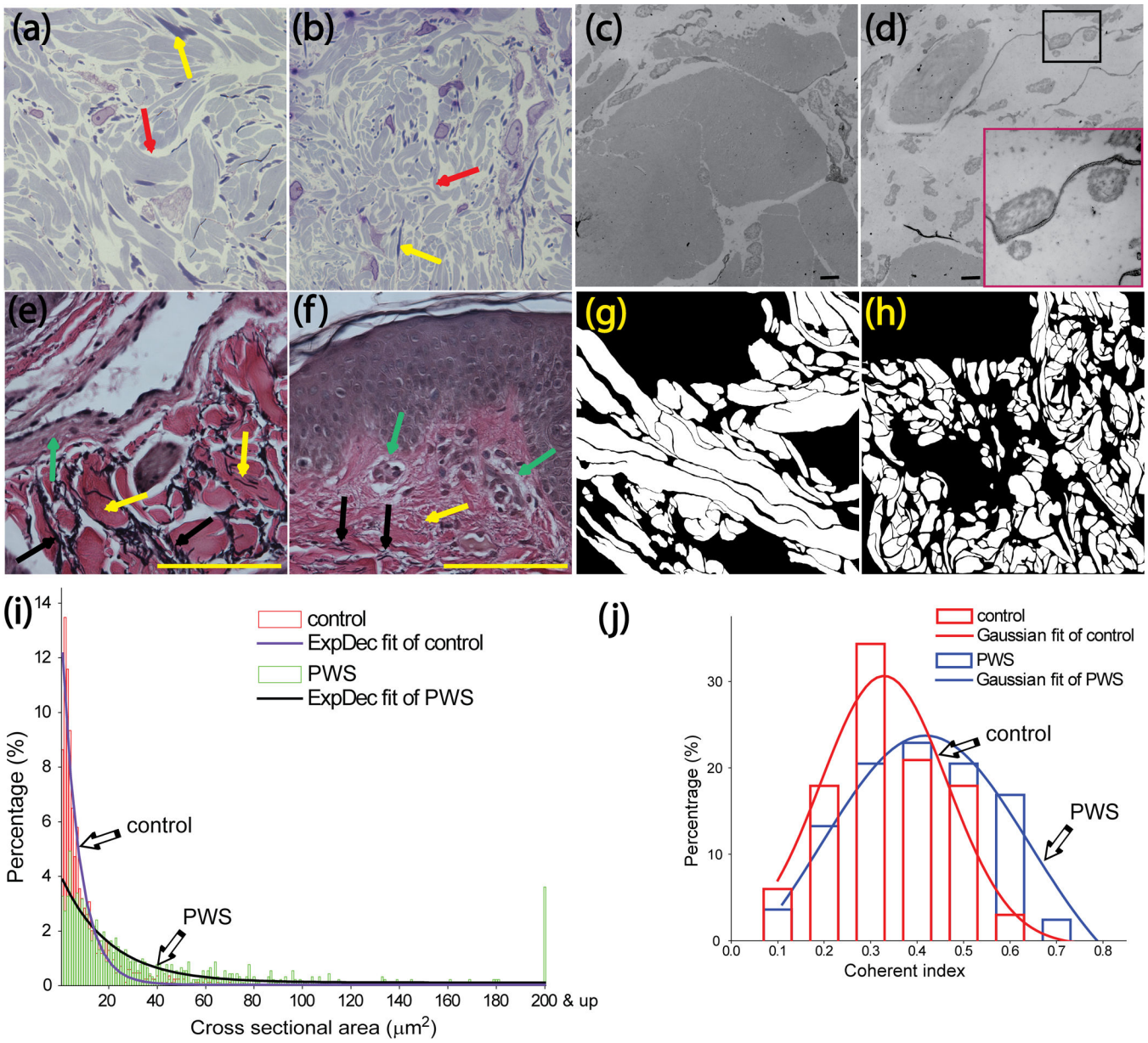

Figure 2.

Hypertrophy and anisotropic orientations of collagen fibers in infantile and early childhood PWS skin.

(a) Hypertrophic collagen (red arrow) and elastic fibers (yellow arrow) in PWS lesions and (b) normal collagen (red arrow) and elastic fibers (yellow arrow) in the control skin from a young child (22-month-old male). Giemsa stain (300×). (c) TEM image showing strikingly hypertrophied collagen fiber and (d) abnormal elastic fibers with marked disorganization. Scale bar: 2 μm (9-month-old female). Red inset represents higher magnification of the boxed area. (e) Hypertrophied collagen (yellow arrows) and elastic fibers (black arrows) and a nearby dilated PWS blood vessel with basement membrane duplication (green arrow); while (f) normal dermal capillaries (green arrows) in the control skin showing normal sizes of collagen (yellow arrow) and elastic fibers (black arrows) in their vicinities. Verhoeff-Van

Gieson stain (400×), scale bar: 100 μm (22-month-old male). (g) Representative outlines showed hypertrophic and anisotropic collagen fibers and (h) normal collagen fibers in the control skin in an infant PWS patient (9-month-old female). (i) Distribution of cross sectional areas of traced collagen bundles (n=848 bundles in the control group and n=919 in the PWS group). An exponential decay (ExpDec) curve was fitted into each data set. (j) The distribution of coherent index of collagen fiber bundles. The outlines of traced collagen bundles were divided into non-overlapped, equal sized squares (10 × 10 μm per square, total n=69 squares in the control group and n=87 in the PWS group). The coherent index was measured from each square using ImageJ plugin OrientationJ (http://imagej.nih.gov/ij/) and their distributions were plotted. A coherence of 1 indicated an ordered and anisotropic pattern while a coherence of 0 indicated a disordered and isotropic pattern. A Gaussian curve was fitted into each data set.